DOI: 10.13009/EUCASS2019-195



# Hypersonic Entry Guidance and Bézier Curves

*Philippe Vernis, Jean-Baptiste Carroy*
*Ariane Group, 78310 Les Mureaux, France*

*philippe.vernis@ariane.group*

## ABSTRACT

Bézier curves have been first defined in the early 60's to help in the computer design of automobile parts. They have many applications in image processing or typography. Because Bézier curves, also termed as B-splines, may represent quite easily any trajectory, they found more recently many applications in the aeronautic and aerospace domains, mainly for unmanned aircraft, trajectory optimisation or some particular guidance problems. One of the difficulties in relying on Bézier curves for designing an atmospheric entry guidance is linked to the large domain of off-nominal flight conditions that may affect strongly the guidance performance. In most of the cases, large environment variations as can be experienced during an atmospheric entry requires an in-flight update of the reference profile to be able to meet the mission requirements expressed in terms of final miss-range and terminal velocity. This paper presents an innovative atmospheric entry guidance designed with a concatenation of 3$^{rd}$-order Bézier curves, enabling an iterative in-flight update process, and the realization of controlled entry trajectories with or without skip but also the avoidance of no-fly zone.

Keywords: *Atmospheric Entry- Bézier Curves- De Casteljau Algorithm- Genetic Algorithms*

## 1. INTRODUCTION

The guided atmospheric entry problem has been widely studied since the 60's but there has been only a few vehicles having experienced it on Earth (mainly the Mercury/Gemini/Apollo, Soyuz or Shenzhou capsules, and for more maneuvering entry vehicles, the Japanese Hyflex demonstrator, the X-37 lifting body and the winged-bodies US and Russian shuttles). On the European side, only the ARD (an Apollo-like capsule) and the IXV (the European Space Agency program of a biconic lifting-body) performed successful one-shot demo-flights in 1998 for the ARD capsule and in 2016 for the IXV lifting body.

Extensive open literature survey concluded that most of the flown guidance schemes were based on the in-flight tracking of a predefined profile, expressed with respect to drag and energy or velocity [1,2,3]. But designing a guidance scheme may be not limited to this class of algorithms, especially for particular entry missions. For instance, a numerical predictor-corrector [4] has been designed within the frame of the ESA-sponsored Skip Entry Program to be able to perform a direct entry or a skip entry with a possible exit of the atmosphere before a final entry. In the other hand, for some other applications, a much more classical but also very simple guidance scheme relying on an adapted Proportional Navigation Law [5] may also be considered. Moreover artificial neural networks, or ANN, whose design process does not need a deep physical approach of the entry problem may be retained to perform a guided entry [9]. In addition, the command parameters may differ from an application to the other: we may use only the bank angle modulation considering that the angle-of-attack profile is predefined (case of a lifting- or winged body) or corresponds to the aerodynamic equilibrium conditions (case of a capsule). But to increase the GNC performance expressed with respect to the miss-range to the targeted point, it can be mandatory to modulate also the angle-of-attack assuming the entry vehicle has enough control means such as flaps, elevons, etc.

DOI: 10.13009/EUCASS2019-195



Recently, a paper presented at the last EUCASS conference [6] focused on the use of the Bézier curves mainly for designing a reference entry trajectory, the application to the entry guidance problem being just lightly addressed. Less recent papers [7,8] introduced an update step based on the current vehicle position to proceed with an on-board computation of the curve, what could be clearly used for guidance purpose. In order to enlarge the in-house available entry guidance algorithms it was then decided to investigate the Bézier Curves-Based Guidance, or BCBG, problem in a three-step approach: definition of the Bézier curves (and internal parameters) matching a reference entry trajectory, solving on-board and at each guidance step an inverse problem yielding the command parameters (angle-of-attack and/or bank angle) from the kinematics induced by the retained Bézier curves modelling, and update of the Bézier curve parameters depending on the potential drift due to command limits and experienced flight dispersions.

The first part of this paper presents Bézier curves and their application to the guided re-entry problem. It introduces a prediction method by on-board solving the inverse problem and an update of the reference trajectory being given the current kinematics of the vehicle. Genetic algorithms are retained to optimize the BCBG internal data. Then, before introducing an area avoidance constraint, the BCBG performance is assessed using unitary and Monte-Carlo simulations focusing on the case where both bank angle and angle-of-attack can be closed-loop controlled.

## 2. Bezier Curves

Bézier curves were introduced by Pierre Bézier, a French automotive engineer, who used them for computer-aided design applications. They are simple polynomial parametric curves allowing easily matching a given shape using control points. The n$^{th}$-order Bézier curve is defined as the following weighted sum:

$$P(\omega) = \sum_{i=0}^{n} P_i B_i^n(\omega) \qquad 0 \le \omega \le 1 \quad \text{with} \quad B_i^n(\omega) = \binom{n}{i}\omega^i(1-\omega)^{n-i}$$

where $P_i$ are the control points and $B_i^n$ are the Berstein polynomials. $\omega$ is referred to as the dimensionless Bézier parameter (or the normalized curvilinear abscissa). Figure 1 illustrates 3$^{rd}$-order Bézier curves with 4 control points.

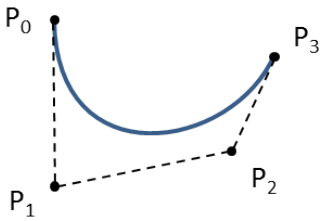


***Fig. 1:*** *3rd-order Bézier curve*

The following properties regarding Bézier curves will be used in this paper:

$$P(0) = P_0$$
$$P(1) = P_n$$
$$\frac{dP}{d\omega}(0) = n\overrightarrow{P_1 - P_0}$$
$$\frac{dP}{d\omega}(1) = n\overrightarrow{P_n - P_{n-1}}$$

From this, the initial and final constraints of position are directly enforced by choosing the initial and final control points $P_0$ and $P_n$. The initial and final constraints on flight path angle, or FPA, and heading are enforced as well by choosing the direction of the nearest control points $P_1$ and $P_{n-1}$.

DOI: 10.13009/EUCASS2019-195



Bézier curves have been studied as a mean to simplify the re-entry problem and lowering the number of parameters in the search of an optimal solution. They are parametric curves allowing easily setting boundary conditions and computing the command using an inverse problem to get the command terms, angle-of-attack $\alpha$ and/or bank angle $\mu$, from the kinematics on the curve. Their application to guidance is intuitive: Bézier curves allow matching any given shape with a limited number of parameters: the control points. Thus, they can be considered as reference trajectory the guidance will try to track. Figure 2 illustrates the Bézier modelling process considering 5 control points $P_0$ to $P_4$ (only the vertical motion is displayed here).

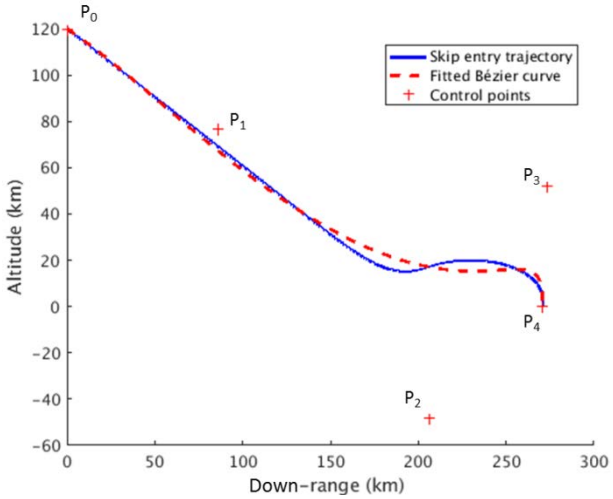


***Fig. 2:*** *Fitting of a re-entry trajectory using a 4th-order Bézier curve*

During the atmospheric entry from Entry Interface Point, or EIP, set at 120 km above ground level (AGL) down to typically Mach 2 gate, or roughly 25 km to 15 km AGL, the vehicle will experience various flight conditions due to its aerodynamic behavior and to the atmospheric properties. For an entry path performing a skip or a large lateral deviation, the number of control points needed to match the reference trajectory may be important [8]. In order to meet a miss-range requirement defined at hypersonic guidance switch-off, the reference trajectory will have to be in-flight updated, tracking the reference trajectory as defined at EIP crossing yielding only poor performance. For limiting the complexity of the Bézier curve-based guidance, it is interesting to define the reference trajectory with less control points. In order to enforce an update process, a property of the Bézier curve that is the possibility to cut in two the curves at a given $\omega_c$ by computing a new set of control points using the De Casteljau algorithm is retained: the restriction of a Bézier curve remains a Bézier curve.

Thanks to this property, the entry path may be designed by a sequence of elementary 3rd-order Bézier curves. And as long as the atmospheric entry does not require any complex trajectory and yields a smooth entry path, the number of Bézier curves can be limited. The main issue modelling the entry path by a succession of Bézier curves will be to define a switching criterion in order to avoid command perturbations and to ensure continuity when passing from one Bézier curve to the next one. Figure 3 displays the fitting of an entry path considering three 3rd-order Bézier curves, the reference entry path being obtained using the Enhanced Skip Entry Guidance, or ESEG [4] in a nominal case.

DOI: 10.13009/EUCASS2019-195



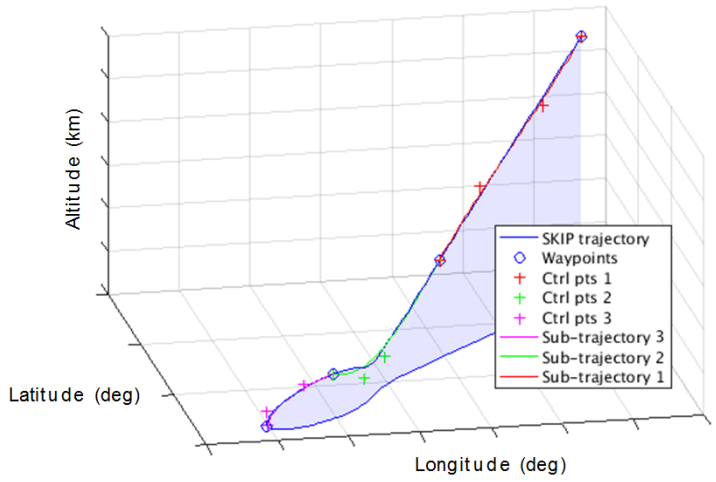


***Fig. 3:*** *Fitting of a skipped trajectory by three 3rd-order Bézier curves*

## 3. Inverse problem

The Bézier curve is just a mathematical form of a trajectory with no direct physical meaning, the $\omega$ Bézier parameter being dimensionless and evolving between 0 (start of the trajectory) and 1 (end of the trajectory). Considering control points defined by geocentric coordinates (radius, longitude and latitude), the coordinates for any point of the curve may be expressed as follow:

$$\begin{pmatrix} r(\omega) \\ \lambda(\omega) \\ \varphi(\omega) \end{pmatrix} = P(\omega) = \sum_{i=1}^{n} B_i^n(\omega) P_i = \sum_{i=1}^{n} B_i^n(\omega) \begin{pmatrix} r_i \\ \lambda_i \\ \varphi_i \end{pmatrix}$$

Once the entry path modelling is done, the first issue is to compute the command (angle of attack $\alpha$ and bank angle $\mu$ or for some cases where only the bank angle $\mu$ can be commanded) from the evolution of the kinematics on the curve. Namely, the classic equations of motion in geocentric frames and spherical coordinates (radius r, longitude $\varphi$ and latitude $\lambda$ for the position, magnitude V, flight path angle $\gamma$ and heading $\chi$ for the relative velocity) are time–dependent:

$$\begin{aligned}
\dot{r} &= V \sin\gamma \\
\dot{\varphi} &= \frac{V}{r} \cos\gamma \cos\chi \\
\dot{\lambda} &= \frac{V}{r \cos\varphi} \cos\gamma \sin\chi \\
\dot{V} &= -g_z \sin\gamma - g_y \cos\gamma \cos\chi - D - \omega_T^2 r \left(\sin\varphi \cos\varphi \cos\gamma \cos\chi - \cos^2\varphi \sin\gamma\right) \\
V\dot{\gamma} &= -g_z \cos\gamma + g_y \sin\gamma \cos\chi + L\cos\mu + \omega_T^2 r \left(\cos^2\varphi \cos\gamma + \sin\varphi \cos\varphi \sin\gamma \cos\chi\right) \\
&\quad + 2\omega_T V \cos\varphi \sin\chi + \frac{V^2}{r}\cos\gamma \\
V\dot{\chi}\cos\gamma &= g_y \sin\chi + L\sin\mu + \omega_T r \sin\varphi \cos\varphi \sin\chi + 2\,\omega_T V(\sin\varphi \cos\gamma - \cos\varphi \sin\gamma \cos\chi) \\
&\quad + \frac{V^2}{r}\tan\varphi \cos^2\gamma \sin\chi
\end{aligned}$$

with D and L the aerodynamic drag and lift acceleration depending from the Mach number $M_a$ the angle-of-attack $\alpha$ and the atmospheric density $\rho$, $\omega_T$ the Earth rotation rate and $g_{x,y,z}$ the components of the gravitational acceleration in the local geocentric frame.

DOI: 10.13009/EUCASS2019-195



Because the Bézier curves are described by the evolution of the Bézier parameter ω, it is necessary to reformulate the entry problem and to rewrite the previous differential equations as ω-dependent. This rewriting step is achieved by introducing the function t(ω). Using this function enables to write the following properties, for any smooth function f:

$$f'(\omega) = \frac{df}{d\omega}(\omega) = \dot{f}(t(\omega))t'(\omega)$$
$$f''(\omega) = \frac{d^2f}{d\omega^2}(\omega) = \ddot{f}(t(\omega))t'(\omega)^2 + \dot{f}\big(t(\omega)\big)t''(\omega)$$

where f′ refers to differentiation w.r.t. the Bézier parameter, and $\dot{f}$ refers to differentiation w.r.t. time. The function t(ω) being a diffeomorphism, such reformulation ensures that the monotony property of the differentiation variable is verified for any problem. This makes possible, for example, trajectory with back turns what could be not be feasible considering the down-range as a differentiation variable[9].

The entry problem can thus be written as ω dependent. As the evolution of the coordinates (r, λ, φ) can be described as Bézier curves, their derivatives can be directly expressed from the Bézier curves equations as follows:

$$\begin{pmatrix} r(\omega) \\ \lambda(\omega) \\ \varphi(\omega) \end{pmatrix} = P(\omega)\,, \qquad \begin{pmatrix} r'(\omega) \\ \lambda'(\omega) \\ \varphi'(\omega) \end{pmatrix} = \frac{dP}{d\omega}(\omega)\,, \qquad \begin{pmatrix} r''(\omega) \\ \lambda''(\omega) \\ \varphi''(\omega) \end{pmatrix} = \frac{d^2P}{d\omega^2}(\omega)$$

From the kinematics equations, the flight path angle γ and the heading χ can be expressed as functions of (r, λ, φ) and their ω-derivatives:

$$\gamma = atan\left(\frac{r'\cos\chi}{r\varphi'}\right) \in \left[-\frac{\pi}{2}\,;\frac{\pi}{2}\right]$$

$$\chi = atan\left(\frac{\lambda'\cos\varphi}{\varphi'}\right) \in\ [-\pi\,;\pi]$$

The variables $\gamma', \chi', t'$ can be expressed as functions of the previously computed variables and of the velocity $V$ by differentiating the kinematics equations. However, it is impossible to find an analytic expression of $V$ because of the dependence of the aerodynamic forces toward the velocity which implies to solve a differential equation. Thus for a practical implementation of this guidance law based on a prediction-update approach, we need to estimate the velocity using a numerical model, such as the Runge-Kutta method, which implies to discretize the problem. This discretization is made on the Bézier variable $\omega$ and the number of points is to be fixed a priori. Then this estimation is periodically updated with the measure of the actual velocity provided by the navigation function of the vehicle.

Once $\gamma', \chi', t'$ are known, the desired lift accelerations on the vertical and lateral axes of the vehicle $a_z = L\cos\mu$ and $a_y = L\sin\mu$ can be computed from the dynamic equations on $\dot{\gamma}$ and $\dot{\chi}$. Here, $a_{ext,z}$ and $a_{ext,y}$ refer to the result of the other exterior accelerations on the vertical and lateral axes of the vehicle:

$$a_z = V\dot{\gamma} - \sum a_{ext,z}$$
$$a_y = V\cos\gamma\,\dot{\chi} - \sum a_{ext,y}$$

DOI: 10.13009/EUCASS2019-195



Finally, the angle of attack α and bank angle μ that will define at each guidance step the command set can be computed from the previous equations:

$$\begin{cases} \alpha = F^{-1}(L, \rho, M_a) \in [0\,;\, \alpha_{max}] \\ \mu = \operatorname{atan}\left(\dfrac{a_y}{a_z}\right) \in [-\pi\,;\pi] \end{cases}, \qquad where\ L = \sqrt{a_z^2 + a_y^2}$$

where F is the model of lift depending from the dynamic pressure, the Mach number and the angle of attack or equivalently from the air volumic mass ρ , the angle of attack α and the Mach number.

In the case only the bank angle can be commanded (the vehicle flies under equilibrium glide conditions [2], or tracking a predefined angle-of-attack profile [1,3], with possible closed-loop updates when large banking are preformed [1]), it is simply determined accordingly to the lift direction or to the vertical or lateral acceleration.
Once the expression of the command set is obtained, another issue in designing an entry guidance with Bézier curves is to enforce the problem constraints enabling finding the control points ensuring the initial (or current) and final constraints on the position.

The initial position derivative can be expressed from the initial velocity, heading and FPA ($V_0$,$\gamma_0$ and $\chi_0$) as follows

$$P'(0) = \begin{pmatrix} r'(0) \\ \lambda'(0) \\ \varphi'(0) \end{pmatrix} = V_0\, t'(0) \begin{pmatrix} \sin\gamma_0 \\ \dfrac{\cos\gamma_0 \sin\chi_0}{r_0 \cos\varphi_0} \\ \dfrac{\cos\gamma_0 \cos\chi_0}{r_0} \end{pmatrix}$$

For a 3rd-order Bézier curve, $P'(0)$ is simply expressed by $P'(0) = 3(P_1 - P_0)$

From that expression, the enforcement of the initial velocity, FPA and heading constraints is ensured by choosing $P_1$ as follow:

$$P_1 = P_0 + k_0 \frac{V_0}{3} \begin{pmatrix} \sin\gamma_0 \\ \dfrac{\cos\gamma_0 \sin\chi_0}{r_0 \cos\varphi_0} \\ \dfrac{\cos\gamma_0 \cos\chi_0}{r_0} \end{pmatrix} \text{ with } k_0 = t'(0).$$

It is possible to find a similar formulation for $P_2$:

$$P_2 = P_3 - k_f \frac{V_0}{3} \begin{pmatrix} \sin\gamma_f \\ \dfrac{\cos\gamma_f \sin\chi_f}{r_f \cos\varphi_f} \\ \dfrac{\cos\gamma_f \cos\chi_f}{r_f} \end{pmatrix} \text{ with } k_f = t'(1) \frac{V_f}{V_0}.$$

$P_1$, $P_2$ and $P_3$ are set by choosing $k_0$, $k_f$, $\gamma_f$ and $\chi_f$. However, the path constraints such as heat flux peak, g-load peak or total heat load are not enforced by this method and can only be verified a posteriori.

The in-flight recalculation of the remaining part of the Bézier curve modelling is performed at a fixed call period accordingly to the best estimates of the kinematics of the vehicle, and the computation of the command is made only for the duration between 2 updates. Due to the discretization issue exposed previously to compute the velocity profile, the command history between 2 updates is given as a look-

DOI: 10.13009/EUCASS2019-195



up-table depending from the Bézier parameter. Using the relation between the Bézier parameter ω and the current time, the current command is eventually obtained by a simple linear interpolation on these tables. The update is obtained using the de Casteljau algorithm to compute $k_0$ and $k_f$ coefficients corresponding to the restriction of the curve from the current position to the final one.

After having fully defined the computation process of the command terms, the last issue is to properly tune the guidance internal data. Up to 3 sub-trajectories modelled by 3rd-order Bézier curves are used to define the entry path. At high altitude, the vehicle flies in a quasi-ballistic mode, the aerodynamic forces being too low to shape the entry path. As a consequence, the first part of the entry cannot be closed-loop controlled, and the number of guidance internal data to set is reduced to 11: $(k_{0,2}, k_{f,2}, r_{f,2}, \lambda_{f,2}, \varphi_{f,2}, \gamma_{f,2}, \chi_{f,2})$ for the second sub-trajectory and $(k_{0,3}, k_{f,3}, \gamma_{f,3}, \chi_{f,3})$ for the third sub-trajectory, see illustration figure 4.

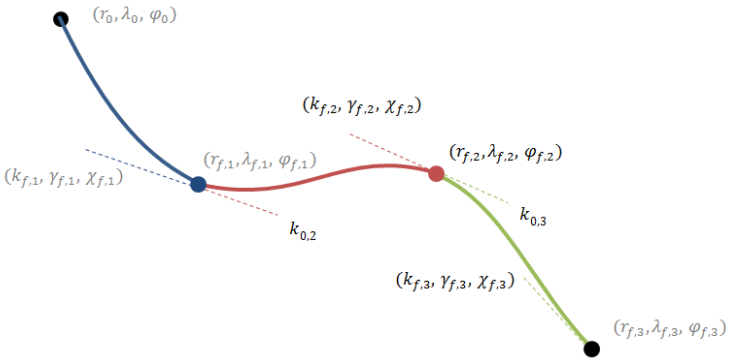


***Fig. 4:*** *Internal Guidance data to be set with GA process*

Among the possible setting process, we retain a genetic algorithm, or GA, based process, this class of optimization process being well suited for problems where we have no a priori knowledge on the behavior of the cost function. In addition, such setting process has already been considered for previous applications [9] giving in each case an accurate setting of the guidance parameters that would have been time-consuming to find using a classic handmade solution.

For this BCBG preliminary analysis, the cost function is defined wrt to a final miss-range criterion, or a mix between final miss-range and terminal velocity. Investigated entry missions being only study cases, path constraints are not included to the cost function. For each scenario, the GA optimization process is made of 3 sub-populations with 30 individuals each, the maximum number of epochs to reach a quite good convergence level is set at 30, and at each step of the GA process, the cost function of an individual is obtained thanks to the simulation of five different off-nominal flight conditions. Figure 5 proposes an example of Bézier curves updates along the entry path (case of an entry path modelled by three 3rd-order Bézier curves). In that case, it is only after crossing the first waypoint that, apart the switching point that are by design taken into account as initial and final point of the current Bézier curve, the updates of the remaining reference trajectory may yield large deviations from one update to the next one shaping slowly the entire entry path.

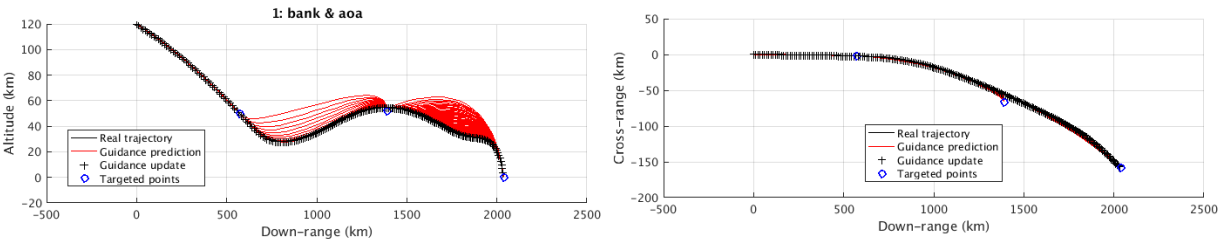


***Fig. 5:*** *Example of Bézier curve updates*

DOI: 10.13009/EUCASS2019-195



## 4. Guidance performance

The ability of this new guidance algorithm to perform an atmospheric entry is assessed considering a notional entry vehicle whose gliding performance can be set by the user accordingly to the type of mission to be tested which is also fully defined by the user. Two command cases are considered: the bank angle and the angle-of-attack can be closed-loop controlled, or only the bank angle.

The retained entry mission is characterized by a shallow entry (FPA around -3 deg), a targeted downrange just above 2000 km and a targeted cross-range of -150 km. During the first part of the entry, the bank angle is adjusted to force a skipped trajectory, the nominal reference entry path being obtained using the Skip Entry guidance [4]. In order to ease the performance assessment, the end of the atmospheric entry is set when reaching the ground, and only a miss-range requirement is considered, the fulfillment of the path constraints being out of the scope of this preliminary analysis.

Considering an update period of 2 s and a guidance call period of 0.2 s, we get the nominal trajectories as displayed on figure 6. Cases 1 and 2 refers to BCBG implementation whereas case 5 corresponds to the ESEG implementation.

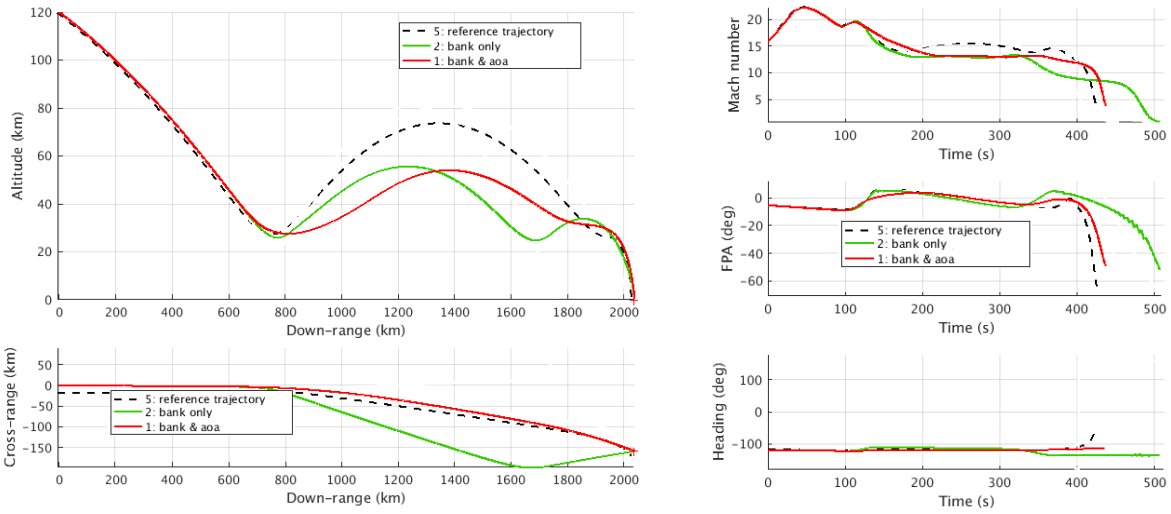


***Fig. 6:*** *ASEG and BCBG trajectory profiles*

We observe that according to the command means but also to the guidance scheme, the shape of the entry path may be drastically different: a large skip (about 50 km vertical deviation) is performed with ESEG, whereas the skip is limited with BCBG, 2 skips being even performed in that case if only the bank angle can be commanded. The top view of the trajectories yields similar profiles for ESEG and BCBG, except when the bank angle only is commanded, the targeted point being reached with a larger cross-range.

DOI: 10.13009/EUCASS2019-195



Figure 7 displays the corresponding time-history of the bank angle and angle-of-attack. We observe different evolutions from one case to the other, especially for the bank angle, the a.o.a evolution of cases 5 and 2 being similar when expressed wrt the Mach number.

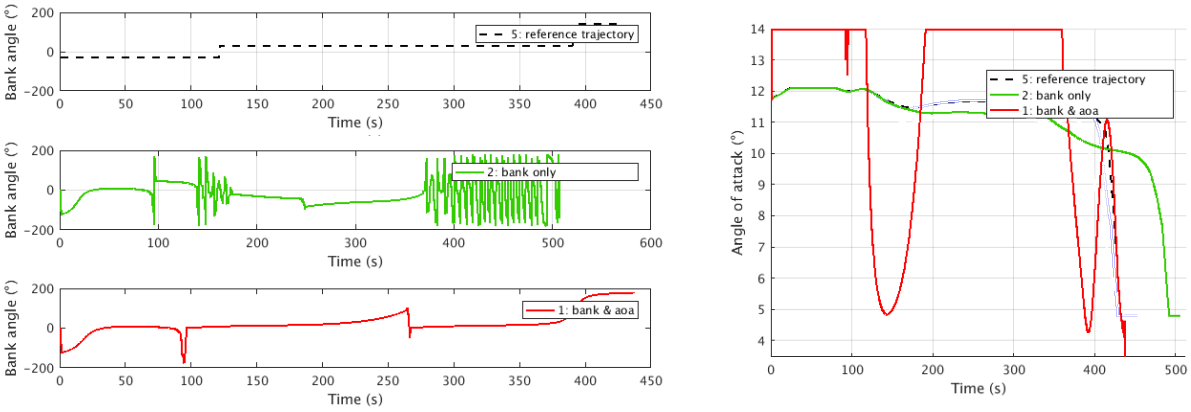


***Fig. 7:*** *ESEG and BCBG bank angle and angle-of-attack profiles*

The peaks that can be observed on the bank angle profile for case 1 are the result of the waypoint crossing triggering the Bézier curves switchings. If needed, they could be smoothed using a simple 1$^{st}$-order filter. For case 2, we observe numerous large oscillations. Here again, those oscillations could be reduced considering a realistic bank angle rate limit, but their occurrence is the result of the limitation of the command to the bank angle only, the vehicle having difficulties tracking the current Bézier curve without rotating along roughly its longitudinal axis.

When running a 1000 cases Monte-Carlo simulation for each of those guidance configurations, we get the statistical results as presented figure 8. In both cases 1 and 2, the final miss-range is very limited, little bit more than 1 km in the worst case. But having the possibility to command both the bank angle and the angle-of-attack yields naturally much better results with a final miss-range around 100 m in the worst case. This performance level is even better than with the original ESEG scheme for which, without any extensive tuning phase, the final miss-range is up to 3 km.

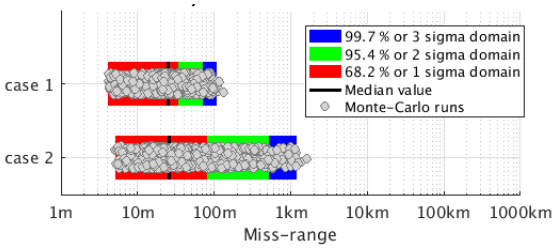


***Fig. 8:*** *BCBG Monte-Carlo results*

At this stage of the analysis, the BCBG scheme may thus yield a good performance in terms of final accuracy. Nevertheless, this analysis will have to be extended to the path constraints which have been ignored here.

DOI: 10.13009/EUCASS2019-195



## 5. Case of area avoidance

As illustrated in the previous section, a Bézier curves-based guidance is able to perform an atmospheric entry with a pretty good final accuracy whatever is the available command: bank angle only or, for a higher accuracy, bank angle and angle-of-attack. Because of its design, it should be able to take into account no-fly zones what is not easily possible to ensure without an extensive tuning phase with all the atmospheric entry guidance schemes developed or implemented until now at ArianeGroup (ARD guidance [1], Enhanced Skip Entry guidance [4] or PN guidance [5], or even ANN entry guidance [10]). In this section, the possibility to avoid a no-fly zone defined by an arbitrary cylinder whose basis is a polygon, is assessed, see illustration figure 9.

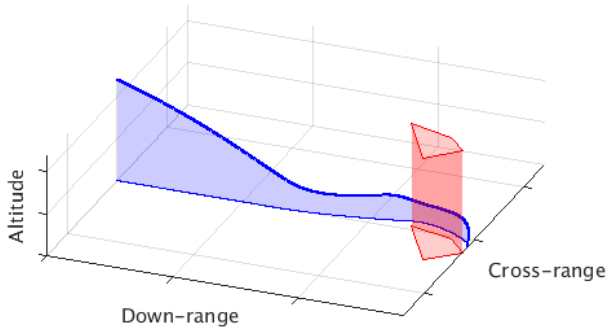


***Fig. 9:*** *impact of aera avoidance on the entry trajectory profiles, case A*

Two command cases are considered: bank angle only (cases 2 and 4) or bank angle and angle-of-attack (cases 1 and 3), and for each case, the cost function of the GA tuning process as exposed previously is defined with respect to the final miss-range only (cases 1 and 2) or to a mix between final miss-range and final velocity (cases 3 and 4). In order to leave some maneuvering margins to the vehicle that has only limited ranging capabilities, we shorten the previous mission, and we locate the forbidden area southwards at the end of the entry path (case A), see left plot on figure 10. With such location, trajectories obtained with command cases 1, 3 and 4 pass just northwards of the forbidden zone, so they would need no real redefinition

Thanks to the GA process that is performed on the expected set of in-flight dispersions, all the ground tracks of the nominal entry trajectories are well shifted away from the forbidden zone with margins left, see right plot of figure 10, highest miss-ranges to the forbidden zone being obtained when both bank angle and angle-of-attack can be controlled.

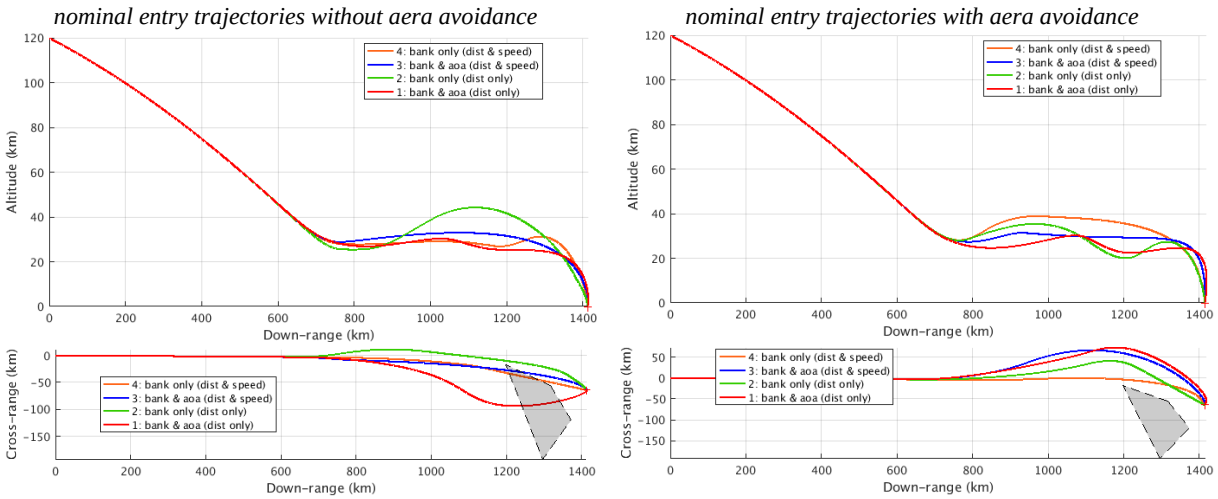

DOI: 10.13009/EUCASS2019-195



***Fig. 10:*** *impact of aera avoidance on the entry trajectory profiles, case A*

When running 1000 runs Monte-Carlo simulations on those different BCBG configurations, no violation of the forbidden zone is to be observed, and the final position accuracies range from less than 50 m (case 3) up to 20 km (case 4), see figure 11.

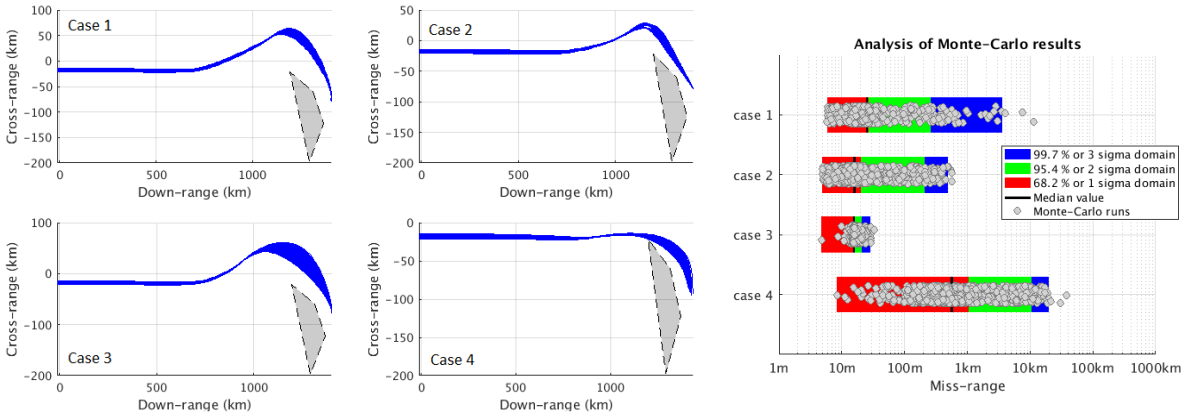


***Fig. 11:*** *aera avoidance Monte-Carlo results, case A*

Moving upwards along the cross-range axis the forbidden zone (case B), see left plot of figure 12, a new GA setting of the guidance data yields margins to the forbidden area only for command case 1 (bank angle and angle-of-attack modulation). For the others command cases, the GA do not converge properly and a limited South violation of the no-fly zone is observed. Giving more weight to the nominal case during the GA process could possibly remove the penetration of the zone, but for comparison purpose, the setting of the GA process is unchanged from one case to the other.

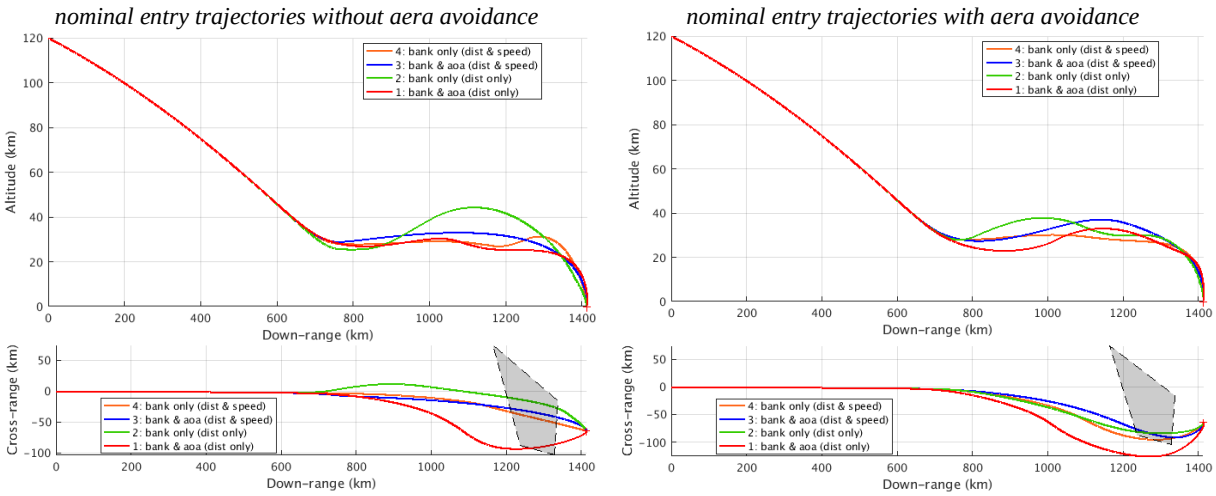


***Fig. 12:*** *impact of aera avoidance on the entry trajectory profiles, case B*

DOI: 10.13009/EUCASS2019-195



When performing 1000 runs Monte-Carlo simulations, we get the results as displayed on figure 13.

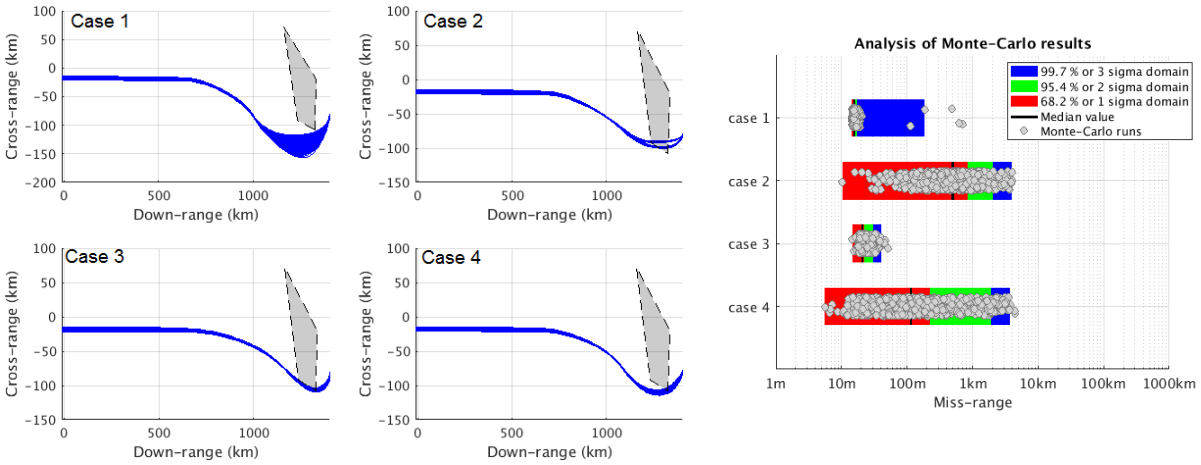


***Fig. 13:*** *aera avoidance Monte-Carlo results, case B*

For this location of the forbidden zone, it is only for case 1 that the no-fly zone is never violated. Cases 3 and 4 yield very limited penetrations (on the south border for case 3, and only around the south corner of the polygon for case 4) whereas the trajectory deviation is not large enough for case 2 to avoid flying in the forbidden zone. But here again, the possibility to act both on the bank angle and the angle-of-attack (cases 1 or 3) helps in meeting the no-fly zone requirement. When looking at the final miss-range, it is also for those simulation conditions that the final miss-range is the best controlled.

## 6. Conclusion

Even if achieved considering a notional entry vehicle whose aerodynamics coefficient are modified to be able to perform the missions under test, as well as arbitrary study cases, this preliminary analysis of designing an entry guidance scheme relying on Bézier curves modelling revealed yet interesting results. The current status is first to model the entry path by a succession of 3$^{rd}$-order Bézier curves, internal data describing this set of Bézier curves being optimized using, for instance, a Genetic Algorithm process, then, to perform in-flight an update of those elementary Bézier curves before computing the current command. By comparison to some existing entry guidance schemes, the Bézier curves–based guidance, or BCBG, can be applied to command configurations for which only the bank angle can be controlled or, what yields the best performance, both bank angle and angle-of-attack can be controlled. Another advantage of this new guidance scheme is that almost any shape of entry trajectory can be considered (direct or skipped entry, with large cross-range or not), for any type of entry conditions as long as the reference entry path can be modelled by a set of Bézier curves. In addition, the BCBG appears well suited to manage flight restrictions such as a no-fly zone. Potential current points to improve and to investigate are that the retained Bézier curve modelling does not take into account any path constraint such as heat flux peak, g-load peak or total heat load. A clearer status will have to be made after a full trade-off between existing guidance schemes applied to realistic missions and vehicles.

DOI: 10.13009/EUCASS2019-195



## REFERENCES

[1] Shuttle Entry Guidance
J.C. Harpold, D.E. Graves
Journal of Astronautics Sciences, 1979

[2] Navigation, Guidance and Control of the Atmospheric Re-entry Demonstrator
G. Pignié, P. Clar, E. Ferreira, L. Bouaziz, J. Caillaud
1st AAAF symposium, Arcachon 1999

[3] GNC for Pre-X Re-entry
P. Vernis, M. Cerf, J. Caillaud, E. Ferreira, S. Guedron
4th AAAF symposium, Arcachon 2005

[4] Accurate Skip-Entry Guidance for low to medium L/D spacecrafts return missions requiring high range capabilities
P. Vernis, F. Spreng, G. Gelly, A. Martinez Barrio
AIAA GNC Portland, 2011

[5] Intercept of Non-moving Targets at Arbitrary Time-varying Velocity
P. Lu
AIAA 1997

[6] Trajectory Optimization of Common Aero Vehicle through Genetic Algorithm aided with Rational Bézier Curve
F. Usman, Z. Ke, A. Mir Soban
7th EUCASS conference, Krakow 2017

[7] Bézier Approximation Based Inverse Dynamic Guidance for Entry Glide Trajectory
T. Rahman, Z. Hao, C. Wanchun
Elsevier, 2013

[8] Near optimal guidance law for descent to a point using inverse problem approach
A. Naghash, R. Esmaelzadeh, M. Mortazavi, R. Jamilnia
Elsevier, 2007

[9] Genetic Algorithm for Coupled RLV Trajectory and Guidance Optimization
P. Vernis, V. Morio, E. Ferreira
ACA congress, Toulouse, 2007

[10] Guided Hypersonic Entry & Artificial Neural Networks – Application to a Hypersonic Entry on Mars
P. Vernis, G. Gelly
3rd EUCASS conference, Versailles 2009

DOI: 10.13009/EUCASS2019-195



## ACRONYMS AND NOTATIONS

| | |
|---|---|
| AGL | Above Ground Level |
| ANN | Artificial Neural Network |
| a.o.a | angle-of-attack |
| ARD | Atmospheric Reentry Demonstrator |
| BCBG | Bézier curves-based Guidance |
| EIP | Entry Interface Point |
| ESEG | Accurate Skip Entry Guidance |
| GA | Genetic Algorithms |
| FPA | Flight Path Angle |
| PN | Proportional Navigation |
| $a_{y,z}$ | acceleration on Y or Z axis |
| $B_i^n$ | Bernstein polynomials |
| D | drag acceleration |
| g | gravitational acceleration |
| $k_{0,f}$ | junction scaling factors |
| L | lift acceleration |
| Ma | Mach number |
| r | radius |
| V | relative velocity |
| r | radius |
| $\alpha$ | angle-of-attack |
| $\gamma$ | flight path angle |
| $\lambda$ | longitude |
| $\mu$ | bank angle |
| $\varphi$ | geocentric latitude |
| $\rho$ | atmospheric density |
| $\omega$ | Bézier parameter |
| $\omega_T$ | Earth rotation rate |
| $\chi$ | heading angle |